NON-NEWTONIAN NATURAL CONVECTION IN A SQUARE BOX SUBMITTED TO HORIZONTAL HEAT FLUX AND MAGNETIC FIELD

Redouane NOURI[1]*,Mourad KADDIRI[1],Youssef TIZAKAST[1], Hamza DAGHAB[1]

[1]Industrial Engineering and surface Engineering Laboratory, FST,Sultan Moulay Slimane University Beni-Mellal, Morocco

[*] Corresponding author; E-mail: redouanech1990@gmail.com

The current work numerically investigates free convection in a square box filled with a non-Newtonian conductive fluid, which is numerically analyzed and is subjected to a steady heat flux at the normal walls, while the horizontal walls are thought of as adiabatic. To examine the impacts of the regulating parameters, including Rayleigh number, Ra*, behavior index,* n*, and Hartman number,* Ha*, on fluid flow and heat transfer, the governing equations are solved numerically by applying the finite volume method (FVM). The results are shown and analyzed in terms of streamlines, isotherms, flow intensity, medium Nusselt, and velocity profiles.*

Key words: Natural convection, non-Newtonian fluids, Finite volume method, magnetic field.

1. Introduction

Natural convection, which produces fluid movement due to density variation engendered by an applied temperature gradient, attracts attention owing to its various applications in the industrial field such as the production of electric power, cooling of electronic components, heat exchangers, solar energy collectors, chemical processes, food processing, and material processing [1, 2].

Given the linked physical phenomena that appeared, scientific researchers concentrated particularly on the impact of the magnetic flux on free convection. The magnetic force caused by the presence of magnetic flux can be exploited in applications such as the control of crystal growth. For example, Vives et al. [3] showed that the consequence of a magnetic flux at the time of the solidification process is characterized primarily by a reduction in superheat escape and an increase in consolidation rate. The focus has been mainly directed towards square cavities, where industrial plants and electronic component cooling are some of the crucial applications that are usually identified by the existence of an intense magnetic flux that reigns in the surrounding space; hence, the usefulness of introducing the magnetic flux in free convection studies. Further, the working fluids are generally non-Newtonian fluids. Many published works investigate the rheological behavior of non-Newtonian fluids in the absence of a magnetic flux [4–7]. Turan et al. [8] demonstrated that the mean Nusselt value augments with enhancing values of Ra and reducing values of the power-law index, while the impact of the Prandtl number Pr is deemed to be negligible. Furthermore, for sufficiently high values of n, the Nusselt number, was found to be equal to unity($Nu = 1$) , as heat transfer is mainly assured by conduction.

In the existence of a magnetic flux, the literature review reveals different works that investigate the consequences of free convection within square cavities filled with Newtonian fluids under varying boundary conditions [9-17]. In all these works, intensifying the magnetic flux is always found to diminish convective fluid flow and heat transfer. However, and as mentioned before, the fluids encountered in the industrial files are mostly non-Newtonian, making the study of natural convection for non-Newtonian fluids under the effect of magnetic field an essential research topic. Yet, the number of investigations conducted does not reflect their importance. For instance, Kefayati [18] used the finite difference lattice Boltzmann (FDLBM), to examine the effect of magnetic flux on natural convection for non-Newtonian power-law fluids in a portion of a heated container. The obtained results showed that extending the behavior index in the nonexistence of the magnetic flux reduces the heat transfer rate, while introducing the magnetic flux diminishes the observed effect of the behavior index on heat transfer. On the other hand, the influence of the behavior index strengthened with increasing the size of the active heated section. Dimitrienko [19] studied the laminar magnetohydrodynamic free convection of a non-Newtonian fluid in a square box under a constant magnetic flux in various directions. This study demonstrated that the angle of inclination has an important influence on flow and heat transfer in addition to the magnetic flux. Liao et al. [20] operated a digital study of free convection induced by a thermally driven flow under the impact of an inclined magnetic flux considering the effects of Rayleigh Ra, Hartmann Ha, and magnetic flux angles. Their findings demonstrated that the direction of the applied magnetic flux had a substantial impact on the streamlines and isotherms furthermore, as the Hartmann number increases, as the applied magnetic field grew stronger, the mean Nusselt Nu and maximum streamline function declined. Makaysi et al. [21] numerically studied the transfer of heat and mass in a square enclosure filled with an electrically conductive non-Newtonian fluid in the presence of an inclined external magnetic flux. The authors observed that the increase in Ha leads to the decrease in the flow intensity, heat, and mass transfer rates dropped for both Newtonian and non-Newtonian fluids. Further, for a weak magnetic flux, decreasing the behavior index n significantly enhanced fluid circulation and heat and mass transfer, while for a great value of Ha, the mentioned effect of n starts to vanish. They also found that the orientation of the applied magnetics flux strongly affected heat and mass transfer. Kefayati [22] investigated the effect of a magnetic flux on free convection in a cavity with a linearly heated wall and filled with non-Newtonian power law fluids. Similarly, they reported the suppressing effect of the magnetic flux on heat transfer rate and the influence of the behavior index. According to the findings of Chtaibi et al. [23], an increase in the power index or Hartmann number has an adverse impact on both flow intensity and heat transfer. These outcomes were obtained through the application of the Boltzmann Lattice Boltzmann Method (LBM) and involved a uniform magnetic field influencing a non-Newtonian fluid in a state of natural convection within an inclined square cavity. In a similar vein, Nouri et al. [24] conducted a numerical assessment of the natural Rayleigh-Benard convection in a square cavity filled with a non-Newtonian fluid whose viscosity is temperature-dependent. Their investigation highlights that the initiation of convection is delayed with higher values of the power index (n) and Hartmann number (Ha). Moreover, it indicates a reduction in both flow intensity and heat transfer as the Hartmann number increases, a trend observed for both Newtonian and non-Newtonian fluids. Notably, at significantly elevated Ha values, heat transfer is predominantly governed by the conduction regime.

The primary objective of this study is to investigate the heat transfer characteristics by free convection within a closed cavity charged with non-Newtonian fluids in the presence of a magnetic flux. Unlike previous research that predominantly considered Dirichlet thermal conditions at the cavity borders, this study specifically aims to explore the influence of Neumann-type thermal boundary conditions in conjunction with the magnetic flux. The existing literature has primarily focused on Dirichlet thermal conditions, leaving a notable gap regarding the consideration of Neumann-type thermal boundary conditions. By incorporating this aspect into the study, we aim to provide a more comprehensive understanding of the thermal behavior within closed cavities with non-Newtonian fluids. The inclusion of a magnetic flux parameter introduces a practical dimension to the investigation. Understanding how magnetic flux interacts with non-Newtonian fluids in closed cavities can have implications in various fields, In summary, this research not only aims to fill a specific gap in the current literature but also strives to advance our understanding of heat transfer in complex systems, providing insights with practical applications and contributing to the broader theoretical framework in fluid dynamics.

2. Mathematical formulation

Figure 1 shows the studied configuration: a two-dimensional square cavity subjected to a horizontal magnetic field and heat flux on the vertical walls while the horizontal walls are insulated. The cavity is filled with Non-Newtonian electically conductive fluids, whose rheological behavior can be characterized by the Ostwald-de Waele power-law model expressed as:

$$\mu_a{}' = K_T \left\{ 2\left[\left(\frac{\partial U\prime}{\partial X\prime}\right)^2 + \left(\frac{\partial V\prime}{\partial Y\prime}\right)^2 \right] + \left(\frac{\partial U\prime}{\partial Y\prime} + \frac{\partial V\prime}{\partial X\prime}\right)^2 \right\}^{\frac{n_k-1}{2}} \tag{1}$$

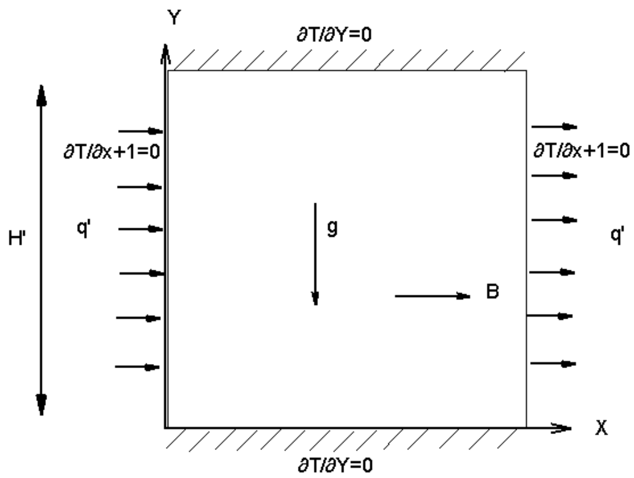

Figure 1. Schematic representation of the cavity with imposed thermal conditions and magnetic field

Where n_k represents the behavior of the flow, and k_T represents the consistency index and which are generally temperature dependent, However, the change of n as a function of temperature is negligible. (nk≈constant = n) with respect to that of kT , This may be calculated using the Frank-Kamenetskii exponential rule:

$$K_T = \mathrm{ke}^{-\mathrm{b}(T'^2 - T_r'^2)}$$

Where b, also known as the thermal dependence coefficient, is an exponent connected to the flow energy activation and the universal gas constant. k is the consistency index at the reference temperature Tr.

for $n = 1$, the behavior is Newtonian, for $0 < n < 1$, the apparent viscosity reduces with the shear rate and the behavior is pseudo plastic (or shears thinning), and for n > 1, the viscosity increases as the shear rate rises, and the behavior is dilatant (or shear-thickening).

Concerning the dimensionless variables, the characteristic scales are as follows: $H', \rho(\alpha^2/H'^2), H'^2/\alpha$, $\alpha/H', q'H'/\lambda$ and α corresponding to length, pressure, time, velocity, temperature and stream function, respectively, are used. As a result, the dimensionless governing equations are given as follows:

2.1. Continuity Equation

$$\frac{\partial U}{\partial X} + \frac{\partial V}{\partial Y} = 0 \tag{2}$$

2.2. Momentum Equation

$$\begin{gathered} U\frac{\partial U}{\partial X} + V\frac{\partial U}{\partial Y} = -\frac{\partial P}{\partial X} \\ +Pr\left[2\frac{\partial \mu_a}{\partial x}\frac{\partial U}{\partial X} + \frac{\partial \mu_a}{\partial Y}\left(\frac{\partial V}{\partial X} + \frac{\partial U}{\partial Y}\right) + \mu_a\left(\frac{\partial^2 U}{\partial Y^2} + \frac{\partial^2 U}{\partial X^2}\right)\right] \end{gathered} \tag{3}$$

$$\begin{gathered} U\frac{\partial V}{\partial X} + V\frac{\partial V}{\partial Y} = -\frac{\partial P}{\partial Y} \\ +Pr\left[2\frac{\partial \mu_a}{\partial Y}\frac{\partial V}{\partial Y} + \frac{\partial \mu_a}{\partial X}\left(\frac{\partial U}{\partial Y} + \frac{\partial V}{\partial X}\right) + \mu_a\left(\frac{\partial^2 V}{\partial X^2} + \frac{\partial^2 V}{\partial Y^2}\right) + RaT\right] \\ -Ha^2 PrV \end{gathered} \tag{4}$$

2.3. Energy Equation

$$U\frac{\partial T}{\partial X} + V\frac{\partial T}{\partial Y} = \frac{\partial^2 T}{\partial X^2} + \frac{\partial^2 T}{\partial Y^2} \tag{5}$$

$$with\ :\quad \mu_a = \left\{2\left[\left(\frac{\partial U}{\partial X}\right)^2 + \left(\frac{\partial V}{\partial Y}\right)^2\right] + \left(\frac{\partial U}{\partial Y} + \frac{\partial V}{\partial X}\right)^2\right\}^{\frac{n-1}{2}} \tag{6}$$

The stream function Ψ is used to study the flux structure:

$$U = \frac{\partial \Psi}{\partial X} \quad , \quad V = -\frac{\partial \Psi}{\partial Y} \tag{7}$$

2.4. Dominant Parameters

In addition to the power-law behavior index n, three other dimensionless parameters appear, namely Rayleigh, Prandtl, and Harman numbers, with their expressions as follows:

$$Ra = \frac{g\beta H'^{(2+2n)}q'}{\left(\frac{K}{\rho}\right)\alpha^n\lambda}\ , Pr = \frac{(K/\rho)H'^{(2-2n)}}{\alpha^{2-n}},\ Ha = B'_0 H'^n\left(\frac{\sigma}{k}\alpha^{1-n}\right)^{\frac{1}{2}} \tag{8}$$

We mention that Pr is fixed at 100 and for the present case, the associated non-dimensional boundary conditions are:

$$U = V = \Psi = \frac{\partial T}{\partial x} + 1 = 0 \qquad For\ x = 0\ and\ x = 1 \tag{9}$$

$$And \; U = V = \Psi = \frac{\partial T}{\partial x} = \frac{\partial T}{\partial y} = 0 \qquad For\; y = 0\; and\; y = 1 \tag{10}$$

2.5. Heat transfer

The Nusselt number, measuring local heat transfer in the horizontal direction, is defined as follows:

$$Nu(y) = \frac{1}{\Delta T(y)}$$

Where: $\Delta T(y) = T(0, y) - T(1, y)$ which represent the dimensionless local temperature difference between the two vertical walls x = 0 and x = 1.

For the average horizontal Nusselt number describing the overall horizontal heat transfer, the following equation is used:

$$Nu = \int_0^1 Nu(y)\, dY \tag{11}$$

2.6. Numerical solution

The preceding Eqs. (2)-(5) associated with the boundary conditions Eq. (10) can be expressed generally as follows [12]:

$$\frac{\partial}{\partial X}\left(U\Phi - \Gamma\frac{\partial \Phi}{\partial X}\right) + \frac{\partial}{\partial Y}(V\Phi - \Gamma\frac{\partial \Phi}{\partial Y}) = S_\Phi \tag{12}$$

With Φ the variable which can be either T, U or V. To find the momentum equation, Γ is replaced by $Pr\mu_a$ a, and for the energy equation it is set to 1 where S_Φ is the source term. To obtain a numerical solution, Eq. 12 must be converted into a linear system, which results in:

$$A_P\Phi_P \quad = A_W\Phi_W + A_E\Phi_E + A_S\Phi_S + A_N\Phi_N + S_\Phi \tag{13}$$

With Φ_P are the variables U, V and T on point P and the equation (13) is the discretized equation that connects the calculation point to its adjacent grid point.

The discretized system is composed of a set of linear algebraic equations that can be quickly resolved using the line-by-line method based on the Thomas algorithm (TDMA) ([26], [27], [28]). The SIMPLE technique [29] is used to solve the connection between velocity and pressure. As for the convergence of the solution, it is evaluated as follows:

$$Max\left(\frac{(\Phi)^{n+1} - (\Phi)^n}{(\Phi)^{n+1}}\right) \le 10^{-6} \tag{14}$$

2.7. Grid size

Tab.1 investigates the variation of the results as a function of the number of grid points in order to identify the optimal mesh size that leads to a satisfactory balance between accuracy and computation time. The results obtained for $Ra = 10^4$, $n = 0.6$, and $Ha = 10$, show that the 120×120 grid is sufficient to accurately simulate the problem at hand.

Table 1: Maximum stream function $|\Psi_{\max}|$ and Nusselt number $\overline{\mathrm{Nu}}$ inside the enclosure for various mesh sizes

Grids	$\overline{\mathbf{Nu}}$	U_{max}	V_{max}	$\lvert\Psi max\rvert$	Dev(%)
80 × 80	2.335	11.038	11.206	2.669	------
120 × 120	2.334	11.053	11.242	2.668	0.32%
200 × 200	2.335	11.054	11.246	2.665	0.112%
300 × 300	2.334	11.055	11.248	2.669	0.149%

2.8. Numerical code validation

We compared our numerical results to previously published ones in order to confirm the numerical code. Tab.2 presents the results in terms of $\overline{\mathrm{Nu}}$ and $|\Psi_{\max}|$ .As can be seen, the agreement is reasonable, with the deviation not exceeding 4.2%, indicating the precision of the adotep numerical code.

Table 2: Validation of current numerical results with previously published research for different n, Pr, Ha, and Ra values.

				Present study		[30]		[31]		[32]	
Ra	Pr	n	Ha	$\lvert\Psi_{max}\rvert$	$\overline{Nu}$	$\lvert\Psi_{max}\rvert$	$\overline{Nu}$	$\lvert\Psi_{max}\rvert$	$\overline{Nu}$	$\lvert\Psi_{max}\rvert$	$\overline{Nu}$
10^6	0.7	1	0	17.07	8.98	17.00	8.90	------	-----	16.75	8.80
			50	10.79	6.39	10.51	6.39	-----	-----	-----	-----
			150	3.91	2.57	3.77	2.64	-----	-----	-----	-----
10^5	$\mathbf{10^2}$	1	0	9.67	4.51	9.75	4.62	-----	4.70	-----	-----
		0.6		28.49	14.99	-----	-----	-----	15	-----	-----
		1.8		3.19	1.57	-----	-----	-----	1.55	-----	-----

3. Results and discussions

3.1. Effects of the Hartmann number on the dynamic and thermal structure of the flow:

Figs. 2 and 3 depict the streamlines for various values of the Rayleigh number (Ra), behavior index (n), and Hartmann number (Ha) with the magnetic flux applied in the x-direction. This analysis aims to examine the flow structure within the square cavities. It is notable that the flow structure undergoes changes in the presence of the magnetic flux (Ha=60), where the streamlines elongate in the vertical direction perpendicular to the magnetic flux. This effect is more pronounced in the central region of the cavity, giving rise to the appearance of two small cells. The observed change becomes more evident as the behavior index (n) decreases and the Rayleigh number (Ra) increases. This alteration can be attributed to the impact of the magnetic force, acting perpendicular to the magnetic flux, on the fluid flow. Additionally, it is worth mentioning that the streamlines become more densely packed and nearly parallel to the adiabatic walls as both Ha and Ra increase.

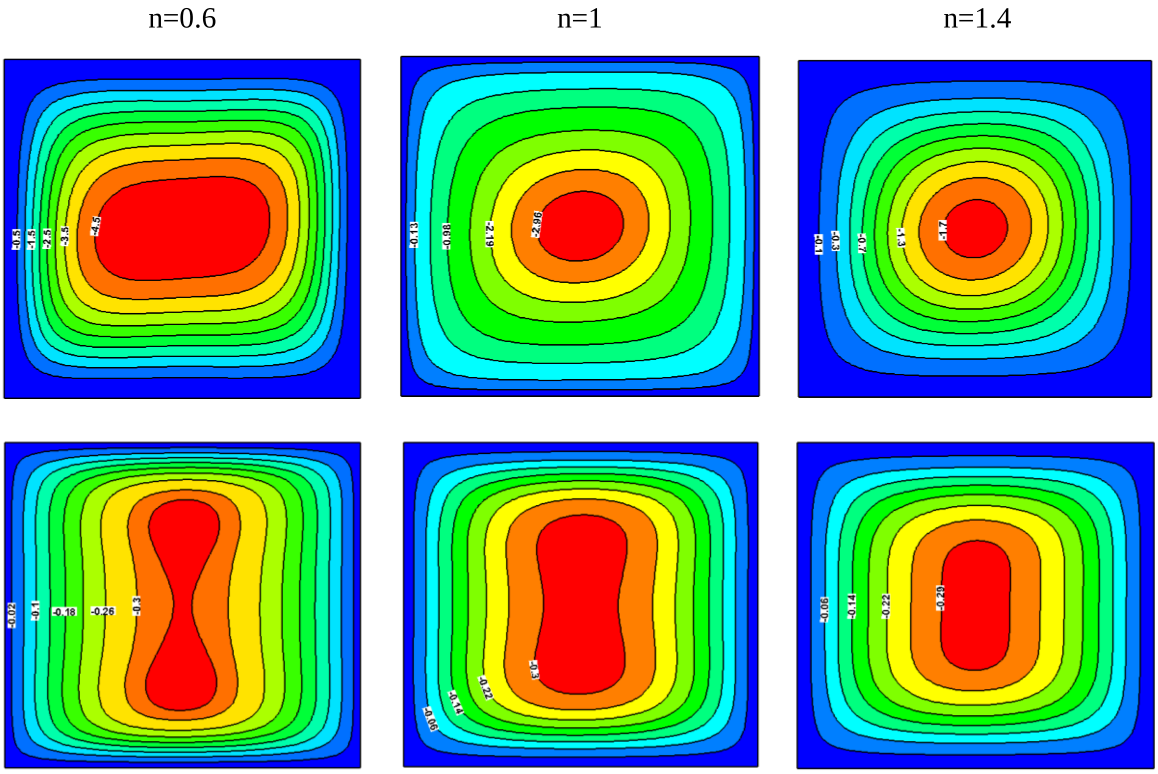

Figure 2. Streamlines for $Ra = 10^4$ and various values of the power-low index n and Hartmann number ($Ha = 0$ (top) and $Ha = 60$ (bottom)).

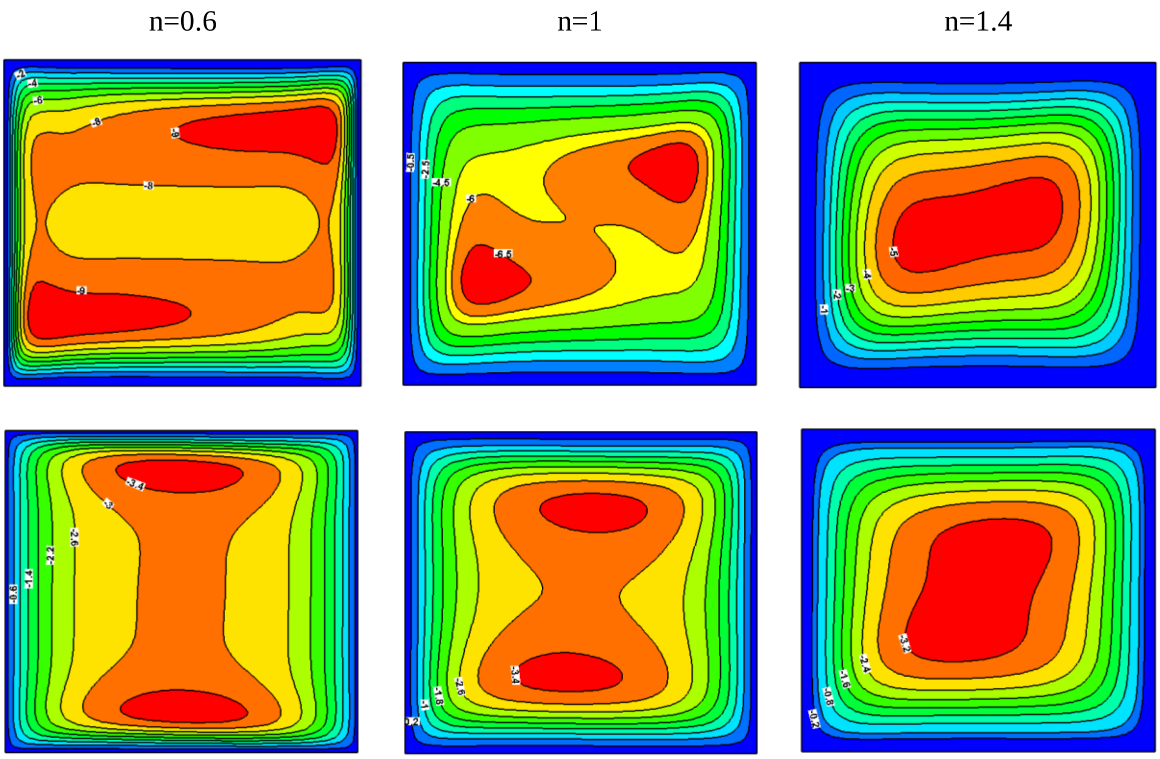

Figure 3. Streamlines for $Ra = 10^6$ and various values of the behavior index n and Hartmann number ($Ha = 0$ (top) and $Ha = 60$ (bottom)).

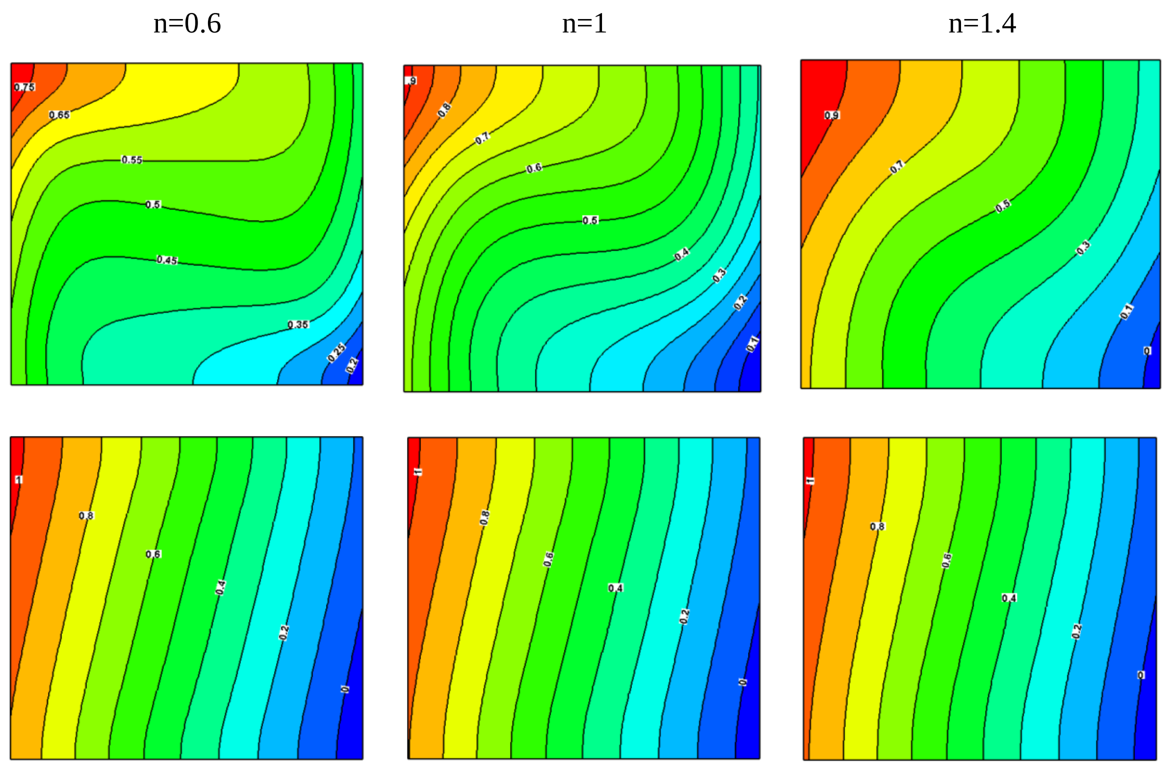

Figure 4. Isotherms for $Ra = 10^4$ and various values of the behavior index n and Hartmann number ($Ha = 0$ (top) and $Ha = 60$ (bottom)).

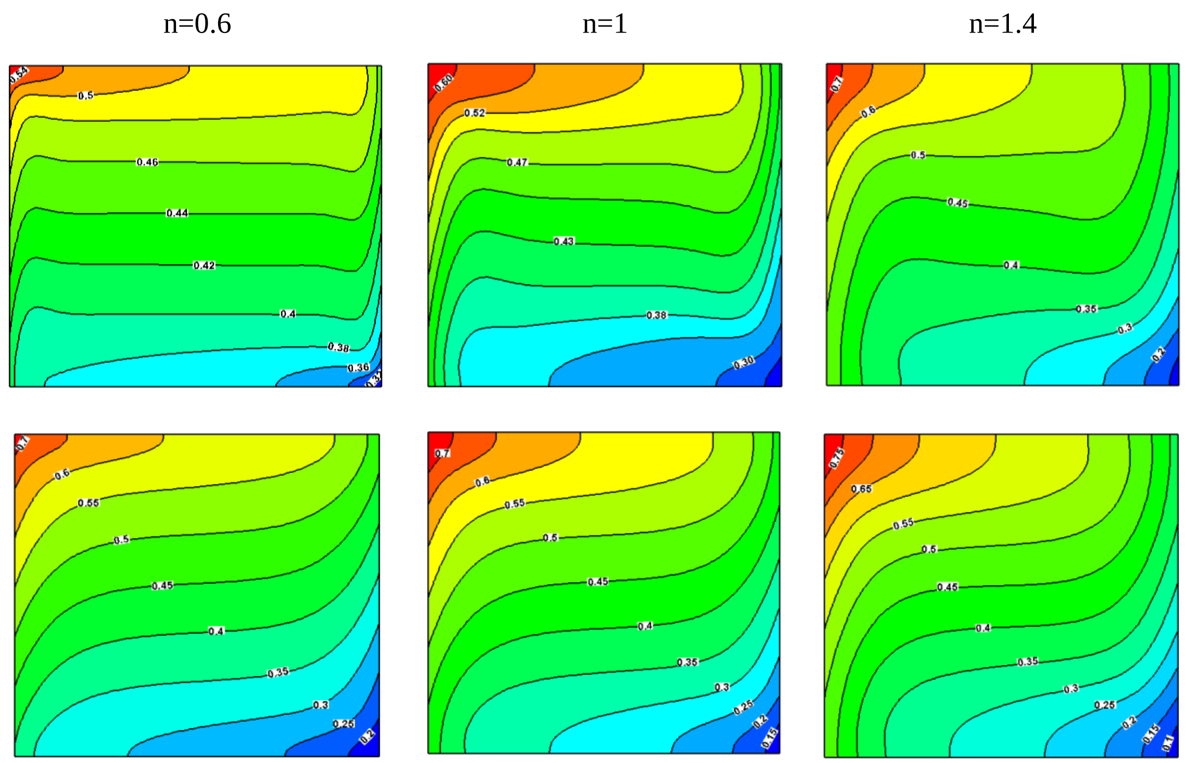

Figure 5. Isotherms for $Ra = 10^6$ and various values of the behavior index n and Hartmann number ($Ha = 0$ (top) and $Ha = 60$ (bottom)).

The observed changes can be interpreted as a result of the combined effects of magnetic attraction, fluid properties, and buoyancy forces. At high Hartmann numbers (Ha), the magnetic field intensifies, promoting the deformation of the flow structure under the Lorentz force with an increase in Rayleigh number (Ra) or a decrease in the behavior index (n). The heightened flow intensity further amplifies the impact of the Lorentz force, leading to the elongation of the central cells and the formation of convective cells near the adiabatic horizontal walls.

These phenomena can be explained by the synergistic effect of the magnetic force and Archimedes' thrust. At sufficiently high Ha values, the flow is predominantly influenced by the magnetic force, which acts perpendicular to the direction of the magnetic field. For instance, when the magnetic field is horizontal in the (x) direction, the magnetic force acts solely in the (y) direction. Considering symmetry, the velocity u dominates along the vertical axis due to v = 0, indicating that the total velocity is nearly parallel to the magnetic field. Consequently, the magnetic force approaches zero since it can counteract the buoyancy effect. As a result, conductive fluids are stretched closer to the horizontal axis.

The corresponding isotherms are presented in Figs. 4 and 5, and they exhibit a tendency to align parallel to the active normal walls as Ha and n increase or Rayleigh number (Ra) decreases. These findings suggest that convective heat transfer weakens while heat conduction intensifies. Consequently, the Lorentz force is enhanced by the magnetic flux, mitigating the convective regime by counteracting the buoyancy force responsible for natural convection, which shows Nevaux that the magnetic field suppresses convection.

3.2. Effects of Hartmann number on flow and heat transfer

Figure 6 displays the profiles of the normal velocity v in the cavity center for various Rayleigh, Hartmann, and behavior index values. The velocity maximum strongly decreases as Ha increases confirming that the magnetic field slows down fluid circulation. The fluid flow intensifies for increasing Ra or decreasing n as natural convection intensifies where the observed diminishing effect of Hartmann number on velocity profiles strengthens. We also notice that the velocity maximum value shifts toward the vertical active walls as Ha and Ra increases and n decreases where the heart region of the enclosure becomes stagnant.

Fig. 7 depicts the evolutions of flow intensity with the regulating Hartmann number, behavior index, and Rayleigh Ra. As expected, the fluid flow intensifies as Ra augments due to the enhanced contribution of buoyancy force. As for the Hartmann Ha, increasing it reduces Ψ_{max} confirming what we mentioned about the magnetic field slowing down fluid circulation. Furthermore, a decreasing power-law behavior index n strengthens fluid flow as the fluid becomes less resistant to motion; however, the magnitude of the effect diminishes as the applied magnetic field further intensifies.

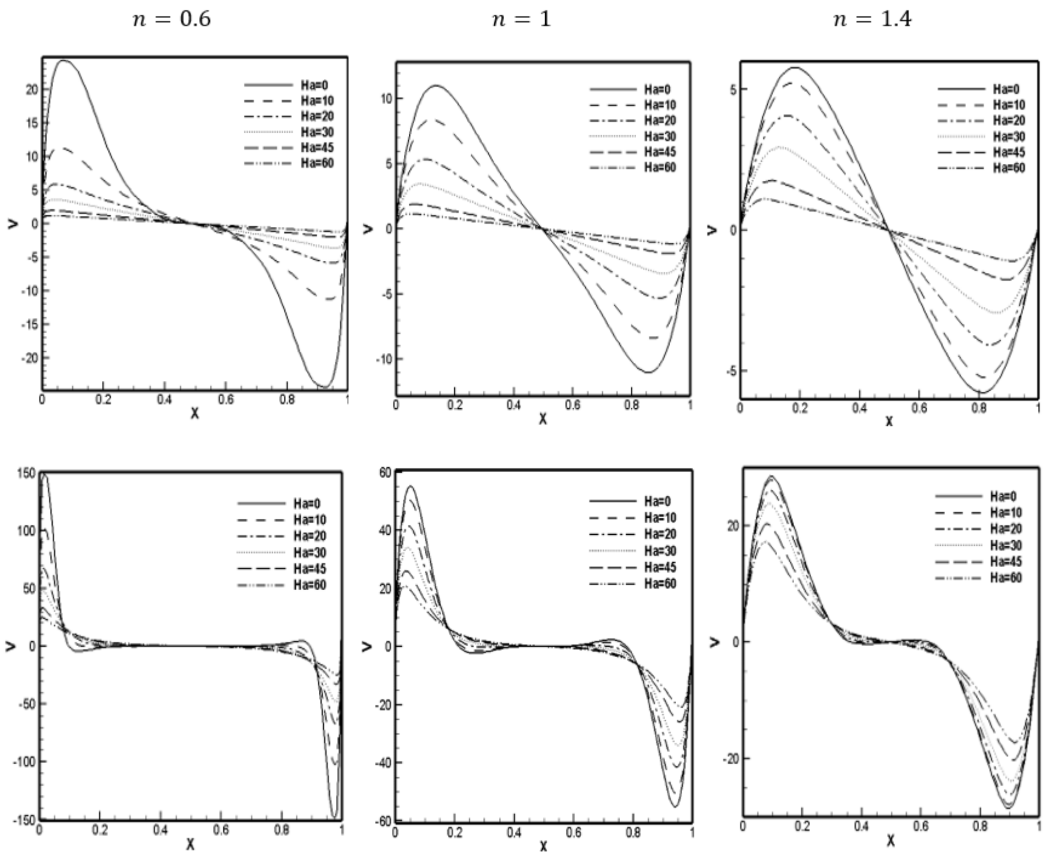

Figure 6. Normal velocity profiles at the center of the cavity $(y = 1/2)$ for various values of the Hartman number Ha, behavior index n, and Raleigh number Ra ($Ra = 10^4$ (top) and $Ra = 10^6$ (bottom)).

The variations of the average Nusselt Nu are illustrated in Fig. 8 for different values of the Hartmann Ha, power-law index, and Rayleigh Ra. First, it is clear that increasing the Rayleigh enhances the influence of decreasing the behavior index on the heat transfer rate. Further, raising Hartmann decreases the average Nusselt Nu with the introduction of the magnetic flux, significantly reducing the observed effect of the behavior index on the heat transfer rate Nu especially for shear-thinning fluids$(n < 1)$.

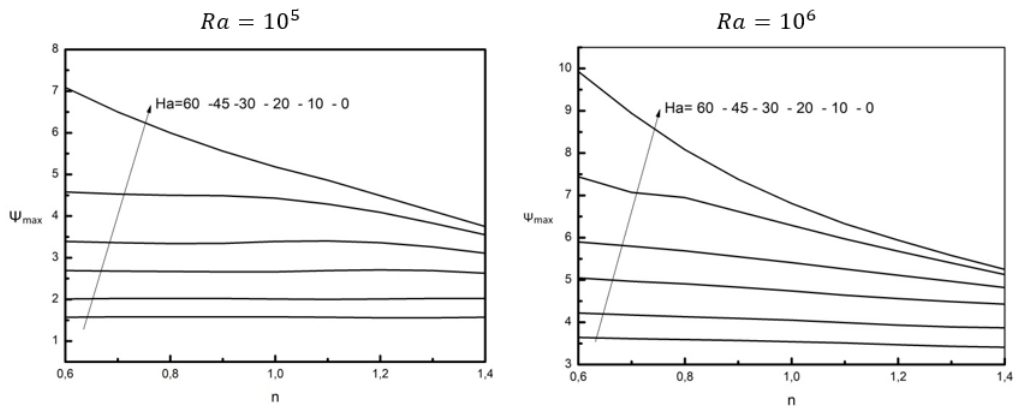

Figure 7. Variations of flow intensity Ψ_{max} for different values of Hartman number Ha, behavior index n, and Rayleigh number Ra.

Fig. 9 shows how the maximum temperature T_{max} varies as a function of Hartmann number Ha, behavior index n, and Rayleigh number Ra. First, increasing Ra decreases the maximum temperature due to the associated strong convective heat transfer. Second, raising the behavior index increases the maximum temperature due to increasing fluid apparent viscosity, which slows down fluid circulation resulting in lower heat transfer. Finally, strengthening the applied magnetic field augments T_{max}, where an increase of Ha from 0 to 60 results in 28% augmentation for $n = 0.6$, while only 8.21% augmentation is observed for $n = 1.4$. Thus, the fluid nature influences the observed magnetic force effect with shear thickening fluids, which are less sensitive to magnetic field presence compared to shear thinning fluids. This is due to the fact that increasing the behavior index n weakens convective fluid flow and heat transfer.

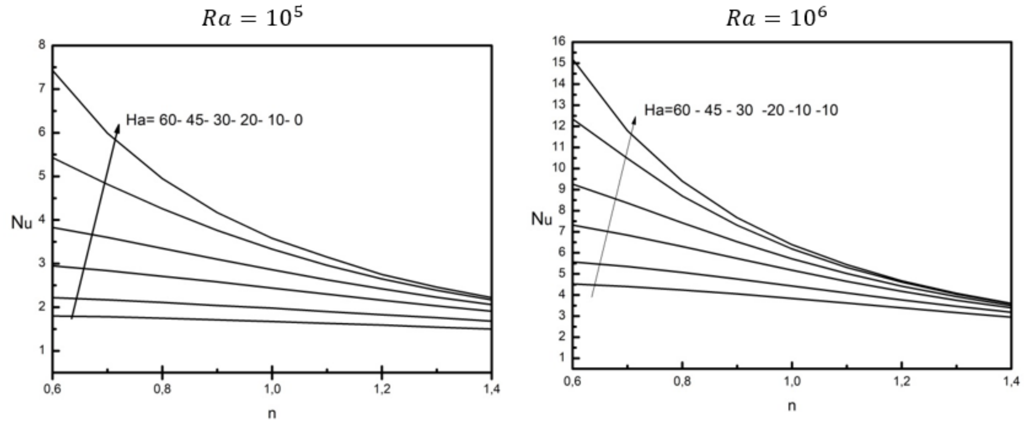

Figure 8. Variations of average Nusselt number Nu for different values of Hartman number Ha, power-law index n, and Rayleigh number Ra.

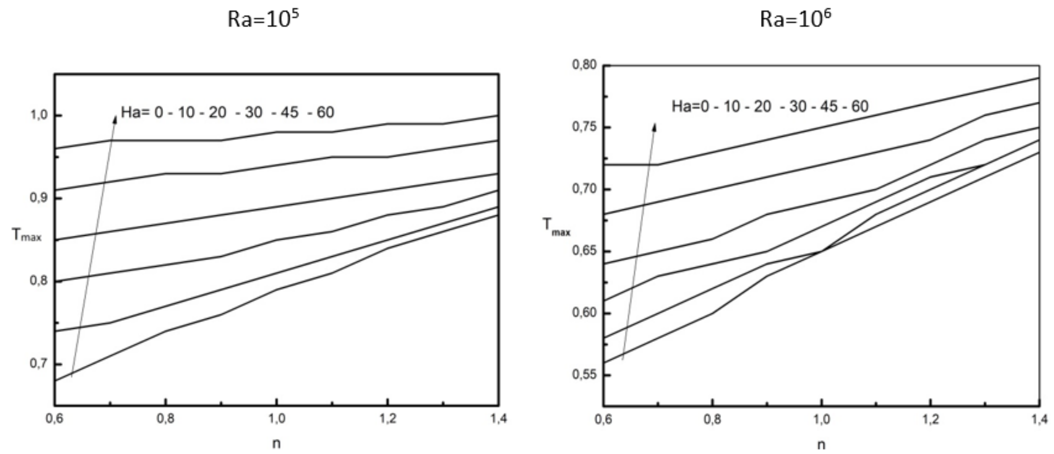

Figure 9. Variations of maximum temperature T_{max} for different values of Hartman number Ha, power-law index n, and Rayleigh number Ra.

4. Conclusion

The present numerical work implements the (FVM) to investigate free convection in a square cavity charged with non-Newtonian conducting fluids and subjected to constant heat flux on the vertical walls and a uniform horizontal external magnetic flux. The examination of governing parameters: Rayleigh number Ra, behavior index n, and Hartman number Ha effects on fluid flow and heat transfer characteristics lead to the following key findings:

- The absence of magnetic flux and the lowering of the behavior index increase the intensity of the flux and the heat transfer, and the maximum temperature decreases.
- The application of the magnetic flux affects the flow structure as the streamlines stretch in the vertical direction perpendicular to the direction of the applied magnetic flux while the isotherms become parallel to the active vertical walls.
- Applying the magnetic flux slows down fluid circulation and decreases the heat transfer rate as the magnitude of the applied magnetics flux, increases.
- The magnetic flux diminishes the enhancing role of the decreasing behavior index.

Acknowledgment

In order to complete this work, we are grateful to the *National Center for Scientific and Technological Research (CNRST-Morocco)* for providing computer resources.

Nomenclature

B_0 – magnetic field strength, [T]
g – gravitational acceleration, [ms^{-2}]
H' – cavity dimension, [m]
Ha – Hartmann number,[–]
k – Consistency index for a power-lawfluid,[Pas^n]
n – Flow behavior index for a power-law fluid,[–]
Nu – average nusselt number ,[–]
P – Dimensionless pressure ,[–]
Pr – Generalised Prandtl number ,[–]
q' – constante heat flux,[wm^{-2}]
Ra – Generalized Rayleigh number,[–]
T – Dimensionless temperature ,[–]
U – Dimensionless normal velocities,[–]
U' – normal velocities,[ms^{-1}]
V – Dimensionless horizontal velocities,[–]
V' – horizontal velocities,[ms^{-1}]
X – Dimensionless normal coordinates,[–]
X' – normal coordinates,[m]
Y – Dimensionless horizontal coordinates,[–]
Y' – horizontal coordinates,[m]

Greek Symbols

α – Thermal diffusivity of fluid,[m^2s^{-1}]
β – Thermal expansion coefficient of fluid,[k^{-1}]
σ – Electrical conductivity of fluid,[sm^{-1}]
λ – Thermal conductivity of fluid,[$wm^{-1}k^{-1}$]
μ_a– Dimensionless effective viscosity,[–]
μ – Dynamic viscosity,[Pas]
ρ – Density of fluid ,[Kgm^{-3}]
ψ – Dimensionless stream function ,[–]

Superscript

' – Dimensional variables.

Subscripts

a – Effective variable.
max – Maximum value.

References

[1] Alegria, Patricia, et al. "Experimental development of a novel thermoelectric generator without moving parts to harness shallow hot dry rock fields." *Applied Thermal Engineering* 200 (2022): 117619.

[2] Hejri, Saeid, and Emad Hasani Malekshah. "Cooling of an electronic processor based on numerical analysis on natural convection and entropy production over a dissipating fin equipped with copper oxide/water nanofluid with Koo-Kleinstreuer-Li model." *Thermal Science and Engineering Progress* 23 (2021): 100916.

[3] Vives, Charles, and Christian Perry. "Effects of magnetically damped convection during the controlled solidification of metals and alloys." *International Journal of Heat and Mass Transfer* 30.3 (1987): 479-496.

[4] de Vahl Davis, G. "Natural convection of air in a square cavity: a bench mark numerical solution." *International Journal for numerical methods in fluids* 3.3 (1983): 249-264.

[5] Ouertatani, Nasreddine, et al. "Numerical simulation of two-dimensional Rayleigh–Bénard convection in an enclosure." *Comptes Rendus Mécanique* 336.5 (2008): 464-470.

[6] Turan, Osman, Nilanjan Chakraborty, and Robert J. Poole. "Laminar natural convection of Bingham fluids in a square enclosure with differentially heated side walls." *Journal of Non-Newtonian Fluid Mechanics* 165.15-16 (2010): 901-913.

[7] Turan, Osman, et al. "Laminar natural convection of power-law fluids in a square enclosure with differentially heated side walls subjected to constant temperatures." *Journal of Non-Newtonian Fluid Mechanics* 166.17-18 (2011): 1049-1063.

[8] Turan, Osman, et al. "Laminar natural convection of power-law fluids in a square enclosure with differentially heated sidewalls subjected to constant wall heat flux." *Journal of heat transfer* 134.12 (2012).

[9] Ozoe, Hiroyuki, and Kazuto Okada. "The effect of the direction of the external magnetic field on the three-dimensional natural convection in a cubical enclosure." *International Journal of Heat and Mass Transfer* 32.10 (1989): 1939-1954.

[10] Venkatachalappa, M., and C. K. Subbaraya. "Natural convection in a rectangular enclosure in the presence of a magnetic field with uniform heat flux from the side walls." Acta Mechanica 96.1 (1993): 13-26.

[11] Alchaar, S., P. Vasseur, and E. Bilgen. "Natural convection heat transfer in a rectangular enclosure with a transverse magnetic field." (1995): 668-673.

[12] Al- Najem, N. M., K. M. Khanafer, and M. M. El- Refaee. "Numerical study of laminar natural convection in tilted enclosure with transverse magnetic field." *International Journal of Numerical Methods for Heat & Fluid Flow* (1998).

[13] Jalil, Jalal M., and Kays A. Al-Tae'y. "The effect of no uniform magnetic field on natural convection in an enclosure." *Numerical Heat Transfer, Part A: Applications* 51.9 (2007): 899917.

[14] Ece, Mehmet Cem, and Elif Büyük. "Natural convection flow under a magnetic field in an inclined square enclosure differentialy heated on adjacent walls." Meccanica 42.5 (2007): 435-449.

[15] Ghasemi, B., S. M. Aminossadati, and A. Raisi. "Magnetic field effect on natural convection in a nanofluid-filled square enclosure." *International Journal of Thermal Sciences* 50.9 (2011): 1748-1756.

[16] Jalil, Jalal M., Kays A. Al-Tae'y, and Sammar J. Ismail. "Natural convection in an enclosure with a partially active magnetic field." *Numerical Heat Transfer, Part A: Applications* 64.1 (2013): 72-91.

[17] Bondareva, N. S., and M. A. Sheremet. "Influence of uniform magnetic field on laminar regimes of natural convection in an enclosure." *Thermophysics and Aeromechanics* 22.2 (2015): 203-216.

[18] Kefayati, GH R. "Mesoscopic simulation of magnetic field effect on natural convection of power-law fluids in a partially heated cavity." *Chemical Engineering Research and Design* 94 (2015): 337-354.

[19] Dimitrienko, Yu I., and Shuguang Li. "Numerical simulation of MHD natural convection heat transfer in a square cavity filled with Carreau fluids under magnetic fields in different directions." *Computational and Applied Mathematics* 39.4 (2020): 1-26.

[20] Liao, Chuan-Chieh, Wen-Ken Li, and Chia-Ching Chu. "Analysis of heat transfer transition of thermally driven flow within a square enclosure under effects of inclined magnetic field." *International Communications in Heat and Mass Transfer* 130 (2022): 105817.

[21] Makayssi, T., M. Lamsaadi, and M. Kaddiri. "Numerical study of magnetic field effect on natural convection heat and mass transfers in a square enclosure containing non-Newtonian fluid and

submitted to horizontal temperature and concentration gradients." *The European Physical Journal Plus* 136.10 (2021): 996.

[22] Kefayati, GH R. "FDLBM simulation of magnetic field effect on natural convection of non-Newtonian power-law fluids in a linearly heated cavity." Powder technology 256 (2014): 87-99.

[23] Chtaibi, Khalid, et al. "Numerical Simulations of the Lorentz Force Effect on Thermal Convection in an Inclined Square Cavity Filled with a Non-Newtonian Fluid." International Days on Thermal Science and Energy. Cham: Springer Nature Switzerland, 2022. 196-206.

[24] Redouane, Nouri, et al. "Rayleigh-Benard Convection Inside Square Cavities Filled with Thermodependent Non-Newtonian Fluids and Subjected to External Magnetic Field." Journal of Advanced Research in Fluid Mechanics and Thermal Sciences 110.2 (2023): 138-156.

[25] N. J. Balmforth and A. Provenzale, Geophysical Aspects of NonNewtonian Fluid Mechanics, vol. 582 of Liberal National Party, Springer, 2001

[26] Patankar, S. (1980). Heat Transfer and Fluid Flow.Hemisphere, New York.

[27] Raghay, S., and A. Hakim. "Numerical simulation of White–Metzner fluid in a 4: 1 contraction." International journal for numerical methods in fluids 35.5 (2001): 559-573.

[28] Van Doormaal, Jeffrey P., and George D. Raithby. "Enhancements of the SIMPLE method for predicting incompressible fluid flows." Numerical heat transfer 7.2 (1984): 147-163.

[29] S.V. Patankar, Numerical Heat Transfer and Fluid Flow, Hemisphere, Washington, DC, 1980

[30] Pirmohammadi, Mohsen, Majid Ghassemi, and Ghanar A. Sheikhzadeh. "The effect of a magnetic field on buoyancy-driven convection in differentially heated square cavity." 2008 *14th Symposium on Electromagnetic Launch Technology*. IEEE, 2008.

[31] Turan, Osman, et al. "Laminar natural convection of power-law fluids in a square enclosure with differentially heated side walls subjected to constant temperatures." *Journal of Non-Newtonian Fluid Mechanics* 166.17-18 (2011): 1049-1063.

[32] de Vahl Davis, G., and IP0538 Jones. "Natural convection in a square cavity: a comparison exercise." International Journal for numerical methods in fluids 3.3 (1983): 227-248.

Submitted 30.10.2023.
Revised 24.01.2024.
Accepted 01.02.2024.